The EMBO Journal Vol. 21 No. 22 pp. 6005–6014, 2002

Altered aggregation properties of mutant γ-crystallins cause inherited cataract

Aileen Sandilands, Aileen M.Hutcheson, Heather A.Long[1], Alan R.Prescott, Gijs Vrensen[2], Jana Löster[3], Norman Klopp[3,4], Raimund B.Lutz[4], Jochen Graw[3], Shigeo Masaki[5], Christopher M.Dobson[6,7], Cait E.MacPhee[7] and Roy A.Quinlan[1,8]

Department of Biochemistry, Medical Science Institutes, University of Dundee, Dundee DD1 5EH, [1]Department of Biological Sciences, Science Laboratories, University of Durham, Durham DH1 3LE, [6]Department of Chemistry, Cavendish Laboratory, University of Cambridge, Madingley Road, Cambridge CB3 0HE, [7]Department of Physics, University of Cambridge, Lensfield Road, Cambridge CB2 1EW, UK, [2]Department of Ophthalmology, Leiden University Medical School, Leiden, The Netherlands, [3]GSF-National Research Center for Environment and Health, Institute of Developmental Genetics, D-85764 Neuherberg, Germany and [5]Department of Biochemistry, Institute for Developmental Research, Aichi Human Service Center, 713-8 Kamiya-cho, Kasguai, Aichi 480-0392, Japan

[4]Present address: GSF-National Research Center, Institute of Epidemiology, D-85764 Neuherberg, Germany

[8]Corresponding author
e-mail: r.a.quinlan@durham.ac.uk

Protein inclusions are associated with a diverse group of human diseases ranging from localized neurological disorders through to systemic non-neuropathic diseases. Here, we present evidence that the formation of intranuclear inclusions is a key event in cataract formation involving altered γ-crystallins that are unlikely to adopt their native fold. In three different inherited murine cataracts involving this type of γ-crystallin mutation, large inclusions containing the altered γ-crystallins were found in the nuclei of the primary lens fibre cells. Their formation preceded not only the first gross morphological changes in the lens, but also the first signs of cataract. The inclusions contained filamentous material that could be stained with the amyloid-detecting dye, Congo red. *In vitro*, recombinant mutant γB-crystallin readily formed amyloid fibrils under physiological buffer conditions, unlike wild-type protein. These data suggest that this type of cataract is caused by a mechanism involving the nuclear targeting and deposition of amyloid-like inclusions. The mutant γ-crystallins initially disrupt nuclear function, but then this progresses to a full cataract phenotype.

Keywords: amyloidosis/γ-crystallins/protein misfolding

Introduction

By the year 2020, the number of blind people in the world will have risen to 45 million (Foster, 1999). The vast majority of these will be caused by untreated cataract, which not only underlines the huge socio-economic impact of this disease, but also identifies a very significant and growing medical problem. In fact, there are some 600 000 new cases every year in the USA and UK alone. The development of novel treatments for cataract are needed, but this is hindered currently by our incomplete understanding of the process(es) of cataract formation in lens cells. Here, we have studied a group of mutations in γ-crystallins that cause inherited cataract.

The eye lens is an organ that retains all its cells for the lifetime of the organism. It is enclosed in a collagen capsule and is bathed in the aqueous humour and so is completely avascular. The lens fibre cells that make up the bulk of the lens are post-mitotic, and the differentiation process involves the complete removal of all cellular organelles including nuclei (Dahm *et al*., 1998), making these fibre cells incapable of protein synthesis, DNA replication and RNA transcription. Although there are many other post-mitotic cells in the body that are equally long lived, none of them survive for decades without these key organelles. The lens fibre cells express a unique set of proteins (Ireland *et al*., 2000) including the γ-crystallins (Graw, 1999), which are a family of structural proteins in the lens. Several autosomal-dominant human cataracts have been identified which are the result of mutations in γ-crystallin (Heon *et al*., 1999; Santhiya *et al*., 2002). In the mouse, there are six distinct γ-crystallin-encoding genes (*Cryga–Crygf*), and mutations in these proteins lead to lens cataract (Graw, 1999). In this study, three established murine models of cataract have been investigated: *Crygb*^{nop} (formerly *Cat2*^{nop}), *Cryge*^{t} (formerly *Cat2*^{t}) and *Cryge*^{elo} (formerly *Elo*) (for a review, see Graw, 1999). All three models have arisen by either a natural frameshift (*Cryge*^{elo}), natural deletion (*Crygb*^{nop}) or radiation-induced nonsense (*Cryge*^{t}) mutations that result in the complete loss of the last (fourth) Greek key motif in domain 2 of the γ-crystallins, which is expected to disrupt the β-barrel arrangement of this domain significantly in each of the mutants. These can be considered as appropriate models for a similar human frameshift mutation in γD-crystallin that also results in the loss of the fourth Greek key motif in domain 2 (Santhiya *et al*., 2002).

The γ-crystallins are most similar to the β-crystallins as they too comprise domains rich in β-sheets arranged in Greek key motifs to form a β-barrel. Both sets of proteins are largely restricted to the lens, although some β-crystallin expression has been reported in the retina (Head *et al*., 1991). Outside the lens, only one protein has been identified thus far that contains βγ-crystallin motifs—a putative tumour suppressor protein, AIM1, that is widely expressed in many different cell types (Ray *et al*., 1997; Teichmann *et al*., 1998). The γ-crystallins are, however, also structurally related to proteins such as IgG and

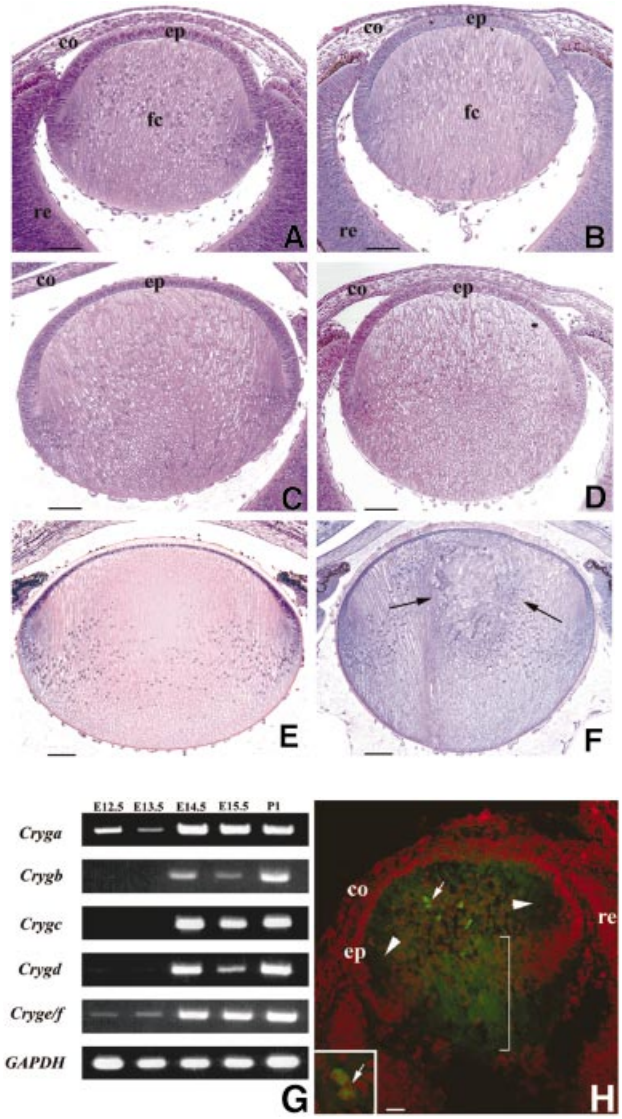

Fig. 1. Histochemical analysis of the appearance of the cataract phenotype in the *Crygb*^{nop} mouse compared with the wild-type from E14.5 to birth (P1). At E14.5, the primary fibre cells fill the lumen of the lens vesicle and the first secondary fibre cells are formed at the lens cortex in both the wild-type (**A**) and the *Crygb* (**B**) lenses. The γB^{nop}-crystallin is first expressed at this developmental time point [see (G) and (H) below]. (**C** and **D**) At E15.5, the first phenotypic changes are obvious. The fibre cells appear swollen and the lens is clearly smaller (D) as compared with the wild-type lens (C). This process continues in the newborn mouse where, in contrast to the wild-type lens (**E**), the centre of the *Crygb*^{nop} lens remains opaque and the primary lens fibre cells become completely disorganized (**F**, arrows). (**G**) All six *Cryg* cDNAs were amplified from E12.5 to P1 from mouse tissues (E12.5–E14.5, head; E15.5, whole eyes; P1, lens). The individual transcripts are indicated along the vertical and the developmental times along the horizontal. The expression of *GAPDH* was used as a positive control. *Cryge/f* and *Cryga* are expressed by E12.5, whereas *Crygb* is first detected at E14.5. (**H**) Polyclonal antibodies specific to γB^{nop}-crystallin (Klopp *et al*., 1998) were used to detect the mutant protein in E14.5 lenses. E13.5 lenses were negative (data not shown), but in the E14.5 lens, γB^{nop}-crystallin (green channel) is present both as nuclear inclusions (arrow and inset) and in the lens fibre cell cytoplasm (bracket) where it is not present as inclusions. This section has been counterstained with propidium iodide (red channel) to locate the cell nuclei. ep, lens epithelium; fc, fibre cell; re, retina; co, cornea. Scale bars = 250 μm in (A–F) and 30 μm in (H).

transthyretin (Getzoff *et al*., 1989). Besides the arrangement of β-sheets in these proteins, the other most notable feature is that both are amyloidogenic (Hurle *et al*., 1994; Lashuel *et al*., 1999), causing disease in both cases (reviewed in Jacobson and Buxbaum, 1991). The data presented here show that the βγ-crystallin motif has similar properties once mutations disrupt the structure and this is the cause of the murine cataracts described in this study.

Results

Mutant γ-crystallins form intranuclear inclusions before the first morphological changes in the lens

We initially examined the events leading up to cataract formation by a comprehensive study of *Cryge*^{t} and *Crygb*^{nop} lenses throughout embryonic development until birth. The data for *Crygb*^{nop} are presented in Figure 1. A section through the mutant lens at embryonic day 14.5 (E14.5; Figure 1B) is comparable with a similar section through the wild-type lens at the same stage of development (Figure 1A): the lens vesicle is completely filled by primary fibre cells and the first secondary fibre cells appear to be formed normally at the equatorial region. By E15.5, however, *Crygb*^{nop} lenses appear slightly smaller than the wild-type, and swelling of the lens fibre cells is observed from the lack of stain in the anterior part of the lens (compare Figure 1D with C). The swelling of fibre cells at the centre of the lens continued until E17.5. Vacuoles become transiently visible at the anterior lateral parts and, although at birth the vacuoles are no longer apparent, the nuclei of the fibre cells are shifted toward the anterior of the lens (compare Figure 1F with E). The degeneration of the lens centre begins at E18.5 and is progressive throughout the life of the animal. By postnatal day 1, an amorphous mass, which can be clearly identified as a cataract, has formed at the core of the *Crygb*^{nop} lens (Figure 1F, arrows). At this stage, however, the anterior epithelium and even the most recently differentiated fibre cells show no obvious morphological abnormalities.

To correlate these morphological changes with the developmental expression pattern of *Cryg* genes in the mouse, RT–PCR was performed. At E12.5 and E13.5, we detected expression of *Cryga* and *Cryge/f* and weak expression of *Crygd*, but detected neither *Crygc* nor *Crygb* (Figure 1G). The latter were first expressed at E14.5, just prior to the first morphological changes at E15.5 for the *Crygb*^{nop} lenses (compare Figure 1D with C). Similar observations were made for *Cryge*^{t}. Expression of γB^{nop}-crystallin was first detected at E14.5 by immunofluorescence microscopy (Figure 1H). The youngest fibre cells, found at the lens periphery, were negative for γB^{nop}-crystallin (Figure 1H; arrowheads), and this region of the lens appears unaffected at all stages of development (Figure 1A–F). In the more central regions of the lens, where γB^{nop}-crystallin is expressed (Figure 1H, green channel), some of the protein accumulates as inclusions (Figure 1H, arrow). These are intranuclear (Figure 1H, inset arrow) as shown by co-localization with the DNA stain, propidium iodide (Figure 1H, inset, red channel). Note that at this stage, not all the γB^{nop}-crystallin is present in nuclear inclusions. Some material was also detected in the cytoplasm, but not as inclusions (Figure 1H, bracket).

γB^{nop}-crystallin expression therefore precedes the first morphological changes in the lens that occur at E15.5.

Immunofluorescence microscopy of sections from *Crygb^{nop}*, *Cryge^{elo}* and *Cryge^{t}* lenses taken at E17.5 indicate that the three different mutations all cause the formation of intranuclear inclusions (Figure 2A–D). These are exclusively nuclear, and no cytoplasmic inclusions nor any cytoplasmic staining in general were seen post-E14.5 in *Crygb^{nop}* lenses, despite the fact that in the wild-type lens γ-crystallins are evenly distributed throughout the cytoplasm of the lens fibre cells and are never seen concentrated in inclusions, whether nuclear or cytoplasmic (Figure 2E, arrows). Using antibodies specific to either γE^{elo}-crystallin (Figure 2C, arrow) or γB^{nop}-crystallin (Figure 2D, arrow), it is clear that the intranuclear inclusions contain the detectable altered γ-crystallin

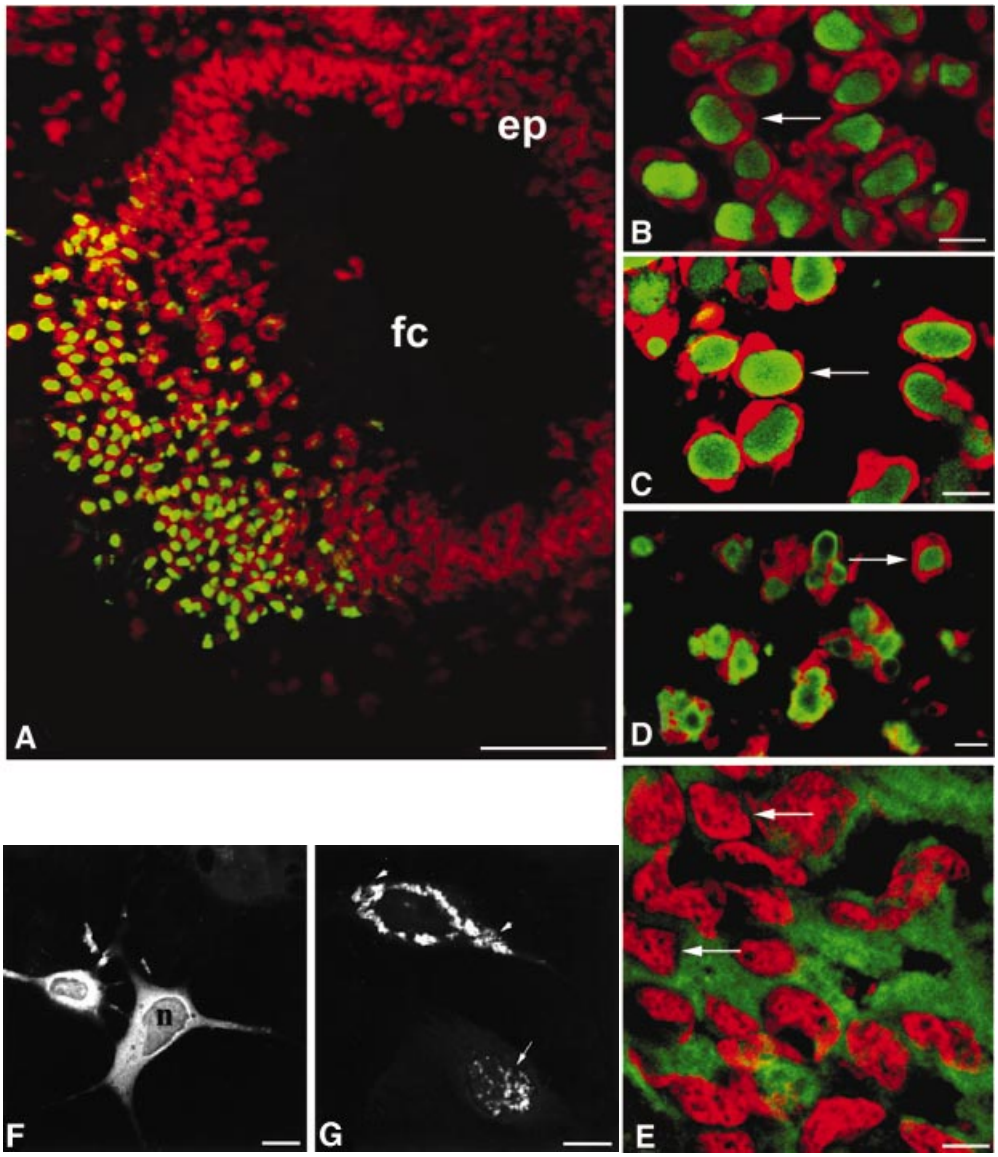

Fig. 2. Nuclear inclusions are common to the three different *Cryg* cataracts. These murine models of cataract have altered γ-crystallin genes that induce similar structural consequences. *Crygb^{nop}* is caused by a replacement of 11 bp by 4 bp in the third exon of γB-crystallin at Ser138, generating a unique hexapeptide sequence at the C-terminus of γB^{nop}-crystallin and truncating the 174 amino acid wild-type sequence at residue 144. A C→G transversion in exon 3 accounts for *Cryge^{t}*, which truncates the protein after residue 143 with no changes to the sequence. *Cryge^{elo}* is characterized by a single base pair deletion in the third exon of *Cryge*, and this also introduces a unique hendecapeptide sequence before a premature termination at residue 145 for γE^{elo}-crystallin. Lenses from E17.5 mice from *Cryge^{t}* (**A** and **B**), *Cryge^{elo}* (**C**) and *Crygb^{nop}* (**D**) were stained (green channel) with polyclonal specific antibodies to all γ-crystallins (A and B), γE^{elo}-crystallin (C) and γB^{nop}-crystallin (D), and also counterstained with propidium iodide (red channel) to highlight the nuclei. Ep, lens epithelium; fc, lens fibre cells. Scale bars = 50 μm in (A) and 5 μm in (B–D). (**E**) Staining of E17.5 lens from a wild-type mouse using polyclonal antibodies that detect all six mouse γ-crystallins (green channel), counterstained with propidium iodide (red channel). Scale bar = 5 μm. Ptk2 cells were transiently transfected with wild-type *Crygb* (**F**) and *Crygb^{nop}* (**G**) both fused to GFP tags to examine the role of the lens environment in nuclear-specific location of the inclusions. Wild-type γB-crystallin is found in both the nuclei (n) and cytoplasm of cells, but does not form protein inclusions. γB^{nop}-crystallin forms both nuclear (arrows) and cytoplasmic inclusions (arrowheads) in transfected cells, the two extremes captured in this image (G). Transfected cells containing both cytoplasmic and nuclear inclusions were a more usual observation. Scale bars = 10 μm.

proteins. In *Cryge*^{t} lenses probed with polyclonal γ-crystallin antibodies, the conspicuous absence of cytoplasmic staining in the mutant lens suggests that the nuclear inclusions also seen in this mutant contained the wild-type γ-crystallins as well as γE^{t}-crystallin.

The lens environment determines the location of the inclusions of altered protein

To explore the importance of the unique environment of the lens to the *Crygb*^{nop} phenotype, γB- and γB^{nop}-crystallin were expressed as green fluorescent protein (GFP) fusions in PtK2 cells, which do not originate from the lens. Inclusions of γB^{nop}-crystallin were formed in both the cytoplasmic and nuclear compartments of PtK2 cells (Figure 2G) whereas the wild-type protein remained distributed throughout the nuclear and cytoplasmic compartments, but not as inclusions (Figure 2F). These data show that inclusion formation *per se* is independent of the lens environment, but the exclusive formation of nuclear inclusions in the lens could reflect the presence of inhibitory factor(s) in the lens cytoplasm.

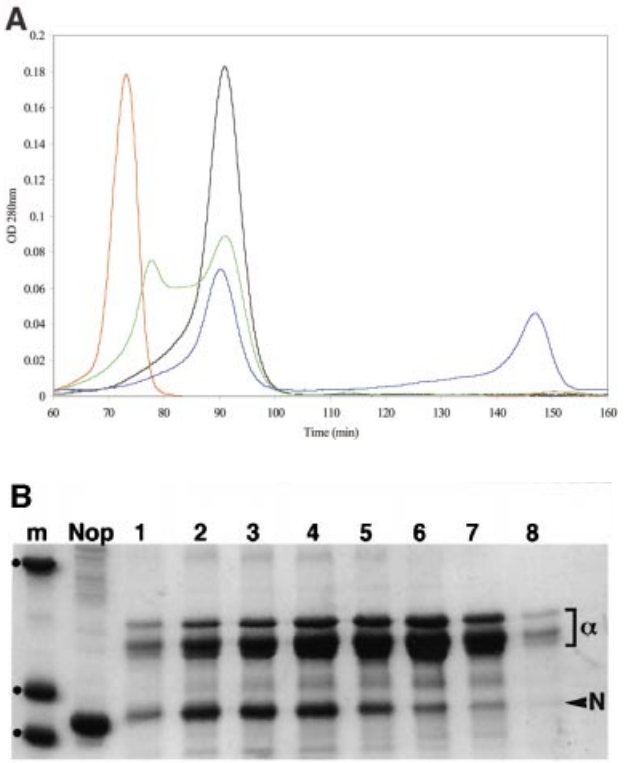

Fig. 3. α-crystallin prevents Crygb^{nop} aggregation *in vitro*. (**A**) Recombinant γB^{nop}-crystallin (red chromatogram) elutes in the void volume of a BioSec size exclusion column indicating aggregation to a size significantly bigger than the molecular weight of the monomeric protein (~20 kDa). α-crystallin (black chromatogram), which oligomerizes *in vivo* to form particles of 800 kDa, elutes after the γB^{nop}-crystallin peak. Wild-type mouse γ-crystallins and α-crystallins elute independently when separated on the same column (blue chromatogram): the γ-crystallins elute after 148 min, equivalent to their mol. wt of 20 kDa, whereas the α-crystallins elute at 91 min. When purified γB^{nop}-crystallin was mixed in equimolar amounts with α-crystallin, two peaks were observed (green chromatogram). One peak has an equivalent elution time to α-crystallin, whilst the other peak is slightly smaller and shifted from the position seen for γB^{nop}-crystallin alone (major peak in the red chromatogram). OD values have been adjusted relative to those obtained for α-crystallin to allow overlay of the different chromatograms. (**B**) The protein content of the two peaks from the green chromatogram was determined by SDS–PAGE, and each peak contains both α-crystallin (α) and γB^{nop}-crystallin (N). This shows that γB^{nop}-crystallin and α-crystallins co-elute, indicating that a protein complex has formed between these proteins. Proteins in fractions after 70, 72, 78, 82, 86, 90, 94 and 98 min are shown in tracks 1–8, respectively. Track M contains marker proteins of 30, 17.2 and 12.3 kDa, indicated by dots. The purity of the starting material γB^{nop}-crystallin is shown (track Nop).

A likely candidate is α-crystallin, which has been shown to inhibit protein aggregation due to its properties as a molecular chaperone (Horwitz, 1992; Hatters *et al.*, 2001). We examined the *in vitro* interaction between α-crystallin and the mutant protein by size exclusion chromatography. In the absence of α-crystallin, recombinant γB^{nop}-crystallin protein eluted in the void volume of the size exclusion column with a retention time of 73 min (Figure 3A, red chromatogram), equivalent to a mol. wt $<2 \times 10^{6}$ Da. This indicated a larger size than even native α-crystallin (800 000 Da) that eluted after 91 min (Figure 3A, black chromatogram). Mixing equimolar amounts of the γB^{nop}-crystallin with α-crystallin gave two peaks, but the γB^{nop}-crystallin peak was shifted and was now not excluded from the column (Figure 3A, green chromatogram). Subsequent analysis of the protein content of these peaks by SDS–PAGE (Figure 3B) indicated that γB^{nop}-crystallin and α-crystallins co-eluted, as both peaks contained both proteins. Both proteins have changed their elution profiles, which now overlap, indicating that mixed complexes have formed. In contrast, when wild-type γ-crystallins were mixed with α-crystallins and subjected to size exclusion chromatography, both proteins eluted as well-separated peaks (Figure 3A, blue chromatogram). They were mixed together in 6 M urea to promote protein unfolding prior to subsequent dialysis into the elution buffer ready for chromatography. The wild-type γ-crystallin peak was well separated from the α-crystallin peak, in line with its expected mol. wt of ~20 kDa. These data suggested that α-crystallin associated with γB^{nop}-crystallin, and prevented the formation of large aggregates that were excluded from the size exclusion column. These data support a role for α-crystallins by possibly preventing the formation of cytoplasmic aggregates by γB^{nop}-crystallin and the other mutated γ-crystallins, leaving the nuclear deposits as the characteristic histopathological feature.

In the lens, the γB^{nop}-crystallin-containing inclusions first appeared at E14.5 in the very central fibre cell nuclei (Figure 1H, arrow). Cytoplasmic staining was also noted, but the cytoplasmic γB^{nop}-crystallin was not present as inclusions. This suggests that other forms of the mutant protein can co-exist with the inclusions, which may be an important consideration for disease mechanisms (Bucciantini *et al.*, 2002). As α-crystallin levels are significantly reduced in nuclei compared with the cytoplasm of cells (Bhat *et al.*, 1999), these data offer an explanation for the formation of nuclear inclusions by the altered γ-crystallins in lens fibre cells.

Intranuclear inclusions of γB^{nop}-crystallin disrupt nuclear function

We next investigated the influence of γB^{nop}-crystallin on cellular metabolism and integrity by staining for lens-specific proteins. The lens-specific intermediate filament

protein CP49 enters the lens fibre cell nuclear compartment only when transcription has been shut down and programmed nuclear destruction has started (Sandilands *et al*., 1995; Dahm *et al*., 1998). Immunofluorescence staining shows that some CP49 had entered the nuclear compartment and was found in the intranuclear inclusions of *Crygb*^{nop} embryo samples (Figure 4A, arrow). Cell apoptosis is stimulated in neurodegenerative diseases in response to inclusion formation (Warrick *et al*., 1998), and the presence of CP49 in the nuclear deposits is also an indicator that apoptotic events have been initiated (Dahm *et al*., 1998) as part of the cataract-forming process. Prox1 is a transcription factor needed to maintain both lens fibre cell differentiation and the expression of *Crygb* and *Crygd* (Wigle *et al*., 1999). In Figure 4B, Prox1 can be seen in all the cell nuclei in a wild-type lens including the central fibre cell nuclei (Figure 4B, arrow). In the *Cryge*^{t} lens, Prox1 is clearly absent from the nuclei of the central fibre cells (Figure 4C, arrow) that also contain the nuclear inclusions. The lens epithelial and early differentiating fibre cells at the lens equator in the *Cryge*^{t} lens still possess nuclear Prox1 (Figure 4C, arrowheads).

The nuclear-specific location of the γ-crystallin-containing nuclear aggregates and the disruption of Prox1 expression suggest that nuclear transcription is disrupted, and this was investigated using established markers of transcription and monitoring the expression of some key lens proteins. Using antibodies to fibrillarin (Figure 5A–D) and coilin (data not shown), it was clear that the transcriptional machinery of E17.5 *Crygb*^{nop} lens fibre nuclei was altered significantly. As has been documented for the bovine lens (Dahm *et al*., 1998), fibrillarin and coilin are sensitive markers of the transcriptional status of lens fibre cell nuclei. Just prior to transcriptional shutdown in these cells, the open floret staining of fibrillarin (Figure 5B, arrow) adopted a closed staining pattern, which coalesced further (Figure 5B, asterisk) as the nuclei break down (Dahm *et al*., 1998). In *Crygb*^{nop} mice, fibrillarin staining was either absent or present in a very diffuse pattern in the nuclei containing intranuclear inclusions (Figure 5D, arrowheads) compared with wild-type embryos at the same stage (E17.5; Figure 5A and B). The aggregates are visible in the nuclei by the exclusion of propidium iodide staining (Figure 5D, arrowheads). The fibrillarin staining also appears irregular in the *Crygb*^{nop} lenses (Figure 5C) compared with wild type (Figure 5A). Closer examination showed that there is a mixture of nuclei with open (Figure 5D, arrow) and closed fibrillarin staining patterns (Figure 5D, asterisk) in the fibre cells adjacent to those containing nuclear inclusions. The most striking effect of the inclusions has been to disrupt the subnuclear organization of the lens fibre cells (Figure 5D, arrowheads), particularly the nucleolar and Cajal body (data not shown) compartments.

These data suggested that lens protein expression patterns are disrupted in the *Cryg* mutants. Analysis of protein levels from E18.5 wild-type (+/+), hetero- (+/N) and homozygous *Crygb*^{nop} (N/N) eyes revealed that levels of the lens-specific intermediate filament proteins, CP49 and filensin, are dramatically reduced (Figure 5E). In contrast, levels of αA-, αB-, β- and γ-crystallin and a third intermediate filament protein, vimentin, appeared to be largely unaffected. These latter genes were all expressed prior to the expression of *Crygb*^{nop}, whilst *CP49* was first expressed around E13 in the mouse, explaining why levels of this protein and filensin are reduced specifically (Ireland *et al*., 2000). These data provide the first evidence of the possible transcriptional effects by the altered γ-crystallins, which clearly impact upon cataract development.

A similar nuclear inclusion phenomenon is observed in Huntington's disease (HD) in humans (DiFiglia *et al*., 1997), and it has been suggested recently that mutant huntingtin also alters transcription as an early event in the pathogenesis of the disease (Dunah *et al*., 2002). This suggests that there could be other similarities between huntingtin- and γB-crystallin-induced nuclear inclusions. The huntingtin-containing nuclear inclusions sequester protein chaperones, such as HSP70 (Suhr *et al*., 2001). The toxic effects of mutant huntingtin can be partially ameliorated by the small heat-shock protein HSP27 (Wyttenbach *et al*., 2002), which is closely related to αB-crystallin. Therefore, we probed thin frozen sections of *Crygb*^{nop} lenses with antibodies to HSP70 and αB-crystallin prior to immunofluorescence microscopy. Both HSP70 (Figure 5F) and αB-crystallin (Figure 5G) were present in the γB^{nop}-crystallin-containing nuclear

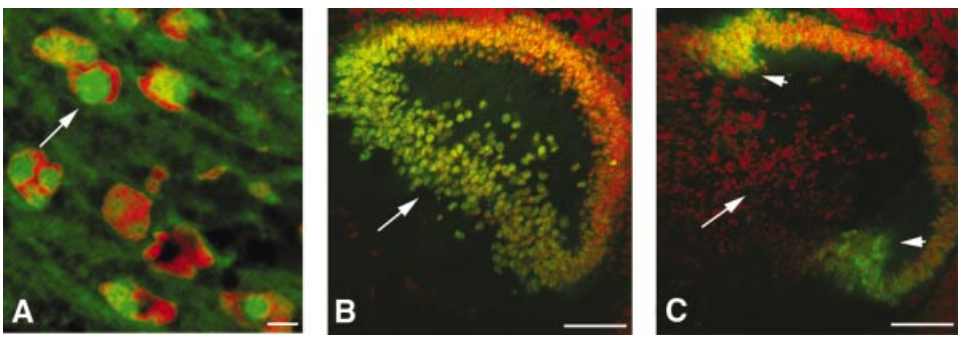

Fig. 4. Identification of lens proteins that associate with the γE^{t}-crystallin and γB^{nop}-crystallin nuclear deposits. (**A**) E17.5 *Cryge*^{nop} lenses were stained with polyclonal rabbit antibodies to CP49 (green channel) and counterstained with propidium iodide to detect chromatin (red channel). The CP49 localizes to the intranuclear inclusions, suggesting that the nuclei have activated those apoptotic-like responses found in normal lens fibre cell differentiation. (**B** and **C**) Cryosections from E15.5 wild-type (B) and *Cryge*^{t} (C) mice were stained with polyclonal antibodies to Prox1 (green channel) and counterstained with propidium iodide (red channel). The nuclei of the wild-type lens, including the central fibre cells (B, arrow), are positive for Prox1, whilst in the *Cryge*^{t} lens, these same nuclei are clearly Prox1 negative (C, arrow). Prox1 expression is lost from all of the fibre cells in the *Cryge*^{t} lens, except for the most recently differentiated cells closest to the lens bow (arrowheads).

inclusions, indicating further similarities between the formation of nuclear inclusions in the two diseases.

γB^{nop}-crystallin containing inclusions in the lens have amyloid-like properties

The resemblance between the intranuclear inclusions formed by the mutant γ-crystallins and the pattern of protein deposition observed in HD prompted us to examine the intranuclear protein inclusions formed by altered γ-crystallins for the presence of amyloid-like fibrils. Amyloid fibrils are extensively ordered β-sheet aggregates observed in a wide range of diseases including HD. The role of the fibrils in pathogenesis has been unclear, although recently it has been proposed that species formed early in the aggregation process are the basis for their inherent toxicity to cells (Bucciantini *et al*., 2002; Walsh *et al*., 2002). This is important in the context of the lens-specific environment which is enriched in α-crystallin, a protein that not only prevents amyloid fibril formation and γB^{nop}-crystallin aggregation (Figure 3A and B) *in vitro* (Stege *et al*., 1999; Hatters *et al*., 2001), but can also increase the toxicity of Aβ (Stege *et al*., 1999). Thin sections from an E18.5 *Crygb^{nop}* lens were stained with Congo red to detect amyloid structures and with haemotoxylin, and viewed by bright field (Figure 6A) and fluorescence (Figure 6B) microscopy. Congo red-positive material, indicative of the presence of amyloid-like structures, was seen in the centre of some of the lens fibre nuclei (Figure 6A, arrows). In such nuclei, the haemotoxylin-positive chromatin was displaced by the Congo red-positive deposits (Figure 6A, arrows). In polarizing light, a few of these positively stained Congo

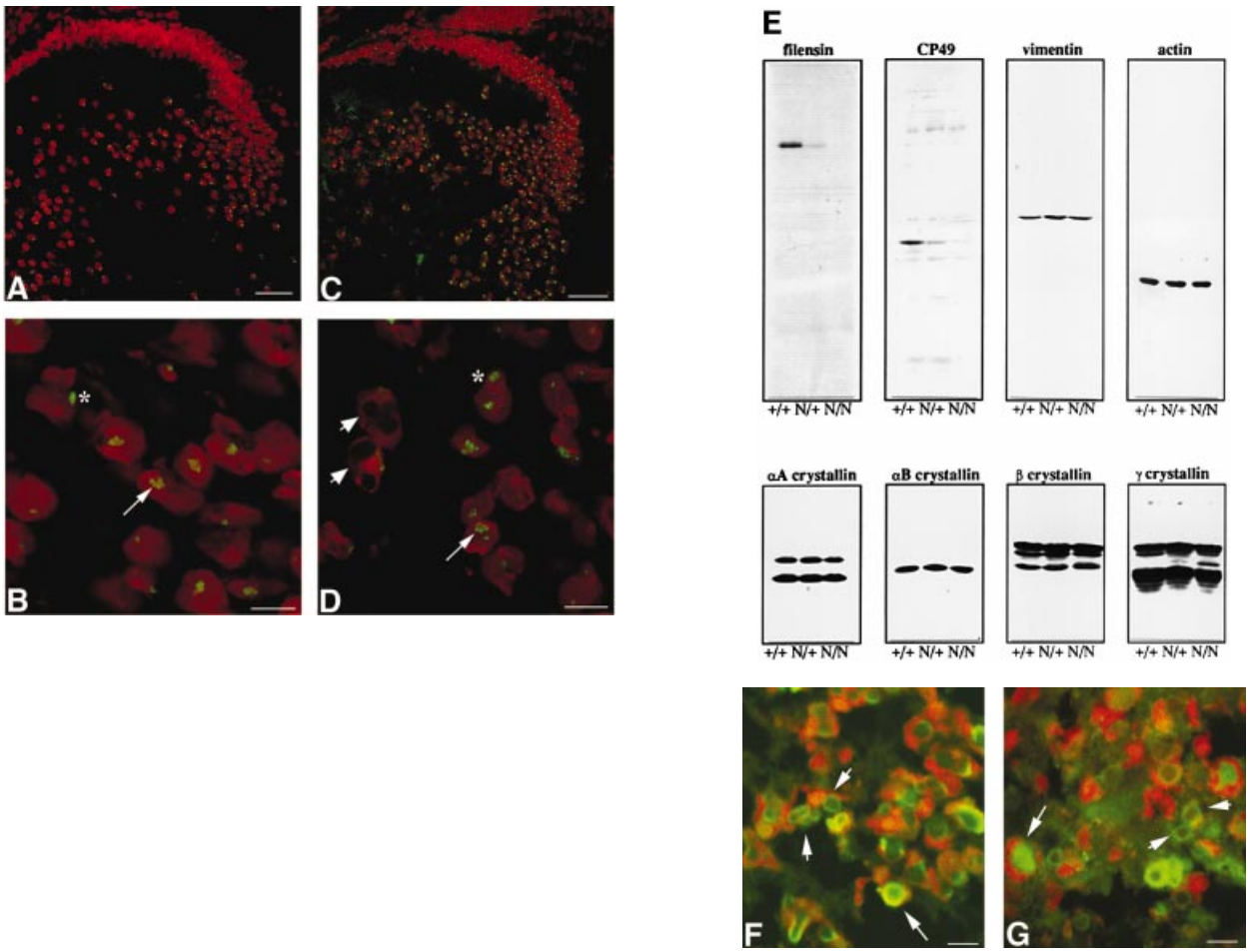

Fig. 5. Wild-type (**A** and **B**) and *Crygb^{nop}* (**C** and **D**) embryos at E17.5 were stained with antibodies to fibrillarin (green channel) and counterstained with propidium iodide (red channel). In the wild-type lens (A), fibrillarin adopts an open floret staining pattern in those nuclei that are transcriptionally active (B, arrow). This pattern then changes in the differentiated fibre cells, resulting in a compact spot(s), indicating that transcriptional activity is reduced (B, asterisk). In the *Crygb^{nop}* E17.5 lens (C), the fibrillarin pattern is punctate when compared with the wild-type lens (A). Many of the nuclei appear to have shut down transcription, as shown by the intense coalesced staining for fibrillarin (C and D, asterisk). Some *Crygb^{nop}* nuclei retain an open staining of fibrillarin (D, arrow), whilst in the nuclei containing prominent γB^{nop}-crystallin inclusions (arrowheads), the fibrillarin is no longer present in foci. This staining pattern was not observed in the wild-type lens. Scale bars = 50 μm in (A and B) and 10 μm in (C and D). (**E**) Immunoblotting with antibodies to vimentin, CP49, filensin, actin, αB-crystallin, αA-crystallin, β-crystallin and γ-crystallin were used to compare levels in E18.5 eye samples from wild-type (+/+), heterozygote (N/+) and homozygote (N/N) embryos. Protein levels appear largely unaffected in all cases except for CP49 and filensin. CP49 and filensin were detected in the N/+ and N/N samples with higher protein loading levels, indicating that they are still expressed although at significantly reduced levels. Cryosections from E17.5 *Cryb^{nop}* mice were stained with antibodies to HSP70 and αB-crystallin (**F** and **G**, respectively; green channel) and counterstained with propidium iodide (red channel). Some inclusions are stained throughout with the antibodies to the protein chaperones (arrows), whereas in some instances only the periphery of the deposits is stained (arrowheads). Scale bars = 5 μm.

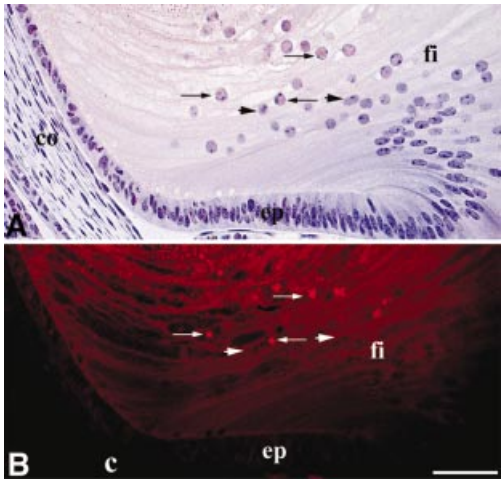

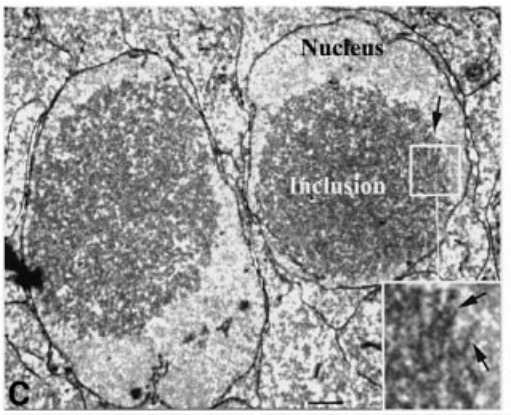

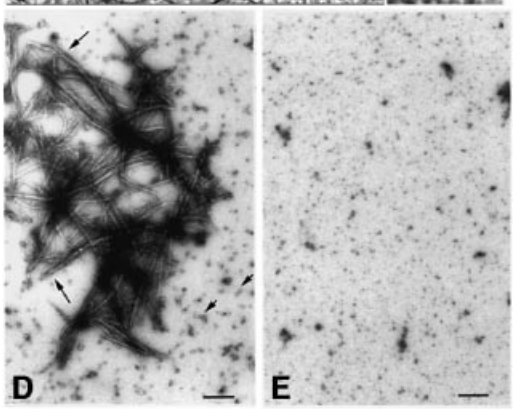

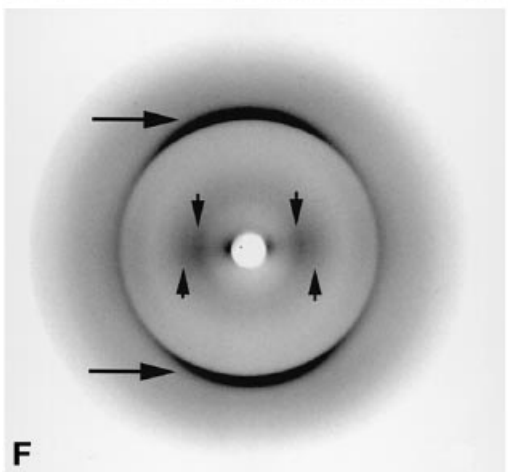

red deposits displayed a just discernable colour shift in polarized light, again characteristic of amyloid deposits (Linke, 2000). Intranuclear aggregates of huntingtin also show variable Congo red staining (McGowan *et al*., 2000), but the most sensitive dye-based method for detecting amyloid deposits utilizes fluorescence of Congo red bound to amyloid (Linke, 2000). With this technique, the γB^{nop}-crystallin-containing nuclear inclusions were quite clearly Congo red positive (Figure 6B, arrows). Other lens fibre nuclei in the section (Figure 6A and B, arrowheads) and the collagen capsule of the lens (Figure 6B, c) did not bind Congo red, as demonstrated by dark field and fluorescence microscopy (Figure 6B and A, respectively), indicating the specificity of the dye for the amyloid-like deposits. Electron microscopy revealed the filament-like substructure of some of these nuclear inclusions in the lens fibre cells of E18.5 *Crygb^{nop}* mice (Figure 6C). Taken together, these data strongly suggest that the intranuclear γ-crystallin-based inclusions contain amyloid-like structures.

γB^{nop}-crystallin forms amyloid fibrils in vitro

In light of these findings, we next investigated whether γB^{nop}-crystallin can form *in vitro* the amyloid-like structures identified by Congo red staining and electron microscopy in the intranuclear inclusions. Electron microscopy of negatively stained recombinant γB^{nop}-crystallin refolded from 8 M urea into 10 mM sodium phosphate buffer pH 7.8 indicates that the mutant protein can form fibrils with a diameter of 6–15 nm (Figure 6D), highly characteristic of amyloid structures formed by other proteins, whilst wild-type γ-crystallins treated similarly do not (Figure 6E). In addition, the amyloidophilic dye thioflavin T (ThT; LeVine, 1999) binds the γB^{nop}-crystallin fibrils in a concentration-dependent manner and shows the characteristic red shift in absorbance maximum from 410 nm to 445–450 nm (data not shown). The X-ray diffraction pattern derived from dried γB^{nop}-crystallin fibrils aligned using a stretch-frame apparatus demon-

Fig. 6. γB^{nop}-crystallin forms amyloid-like structures. (**A** and **B**) E18.5 lens from *Crygb^{nop}* mice, stained with Congo red and haemotoxylin and viewed by bright field (A) and fluorescence microscopy (B). Only those nuclei near the centre of the lens are positive (arrows), but those in the outer lens fibre cells (fi), the lens epithelium (ep) and surrounding tissues (e.g. the cornea; co) are all negative (B, arrowheads). The lens capsule (B; c) is also negative. Adjacent sections were stained with γB^{nop}-crystallin-specific antibodies to confirm that the Congo red-positive nuclear deposits contained γB^{nop}-crystallin. Scale bar = 50 μm. (**C**) An example of a filamentous substructure of a nuclear inclusion found in lens fibre cells of E18.5 *Crygb^{nop}* mice as seen by electron microscopy. The fibrillar-like substructure of the inclusions is indicated (arrow). Notice the clear fibrous substructure of this region of the inclusion in the insert (C; insert, arrows). This region was located at the edge of one of the inclusions and, as such individual filaments are not so obvious in the centre of the inclusion, it suggests that either the filamentous material 'matures' within the inclusion or that there is a degree of polymorphism in the aggregated forms of γB^{nop}-crystallin. Scale bar = 500 nm. (**D**) Dialysis of recombinant γB^{nop}-crystallin into 10 mM sodium phosphate pH 7.8, 1 mM EDTA results in the formation of both fibrils (arrows) and small rod-like particles (arrowheads), possibly due to morphological variation and/or the presence of intermediates in fibril formation. (**E**) Wild-type γ-crystallins do not form fibrils under these conditions. Scale bars = 200 nm. (**F**) X-ray diffraction of the fibrils assembled from γB^{nop}-crystallin indicates formation of the typical 'cross-β' X-ray diffraction pattern characteristic of amyloid fibrils. Reflections can be observed at 4.7 Å (arrows) and two reflections at 10.7 and 12 Å (arrowheads).

strates reflections diagnostic of the 'cross-β' structure characteristic of amyloid fibrils (Figure 6F). The meridional reflections at 4.7 Å represent the hydrogen bonding distance between the β-strands, and the reflections observed at 10.7 and 12.0 Å represent the distance between adjacent β-sheets arrayed perpendicular to the long axis of the fibrils. These data show that γB^{nop}-crystallin forms amyloid fibrils *in vitro* and, in combination with the data presented in Figure 6A and B, indicate that the mutant γ-crystallins in this study form aggregates that lead to intranuclear amyloid-like deposits and eventually to cataract.

Discussion

The formation of amyloid fibrils by the γ-crystallins in mouse models of cataract is analogous to protein deposition in a number of human diseases where mutation of the protein destabilizes the native structure, promoting refolding into amyloid fibrils. The specific role of amyloid deposits in human disease is still being debated (Pepys, 2001; Bucciantini *et al*., 2002; Walsh *et al*., 2002) and similar questions are being asked of other inclusion-based diseases such as amyotrophic lateral sclerosis (Bruijn *et al*., 1998) and the glutamine repeat disorders (Sisodia, 1998) which include HD. Here, it is clear that the γ-crystallin inclusions precede the first morphological changes in the *Crygb^{nop}* lens fibre cells (Figure 1). Our data also indicate that γB^{nop}-crystallin is present in both inclusion and non-inclusion forms (Figure 1H) prior to the first phenotypic changes, contributing to the debate over the relative importance of the soluble aggregates compared with the inclusions to cell toxicity (Bucciantini *et al*., 2002; Walsh *et al*., 2002). Minimally, the data here show the altered γ-crystallins have gained a function that is toxic, initiating a series of events that lead to cataract.

The data we have presented suggest that one of the toxic consequences of γB^{nop}-crystallin expression is the disruption of transcriptional processes. For instance, we observed the dramatic reduction in the expression of some key lens fibre cell proteins (Figure 5E) and a general shut down in transcription as revealed by fibrillarin staining (Figure 5A–D). There is also the loss of Prox1 from the central fibre cells from *Cryge^{t}* lenses (Figure 4C), an important transcription factor required for maintaining fibre cell differentiation (Wigle *et al*., 1999). These changes are an integral part of the cascade of events that culminate in the formation of cataract, providing an interesting parallel with the neurodegenerative disease, HD. Here, huntingtin, which also forms characteristic nuclear inclusions, causes transcriptional effects that are early events in the disease (Dunah *et al*., 2002; Kegel *et al*., 2002). Cataract, like HD, is a progressive disease, but our data suggest that the loss of nuclear function is one of the events at the start of this process.

The studies here have concentrated on the frameshift murine *Cryg* mutations leading to substantial truncation of full-length γ-crystallins. The recent discovery of a frameshift mutation in γD-crystallin (Santhiya *et al*., 2002) that results in a truncated protein lacking the last Greek key motif and is the cause of one inherited human cataract suggests that the *Cryg* mutants described here are important animal models of human disease. In humans, it has been proposed that the formation of cataract in some of these cases is the result of spontaneous crystallization of the mutant protein (Pande *et al*., 2001), and indeed mutation of surface residues promotes crystallization of some proteins (Kmoch *et al*., 2000). The frameshift mutations studied herein, however, should be treated as a protein folding disorder rather than a native state aggregation process, as the severity of the mutations involved is unlikely to result in a fully folded protein capable of crystallization. We therefore suggest that some hereditary forms of cataract involving mutations that are able to disrupt the native structure of the γ-crystallin significantly may involve the aggregation and resulting deposition of the misfolded protein as amyloid-like inclusions.

Materials and methods

Histological investigations

Embryos of timed-pregnant *Crygb^{nop}* (formerly *Cat2^{nop}*) mice were bred at the GSF research centre. Either C3H/E1 or (102/E1 × C3H/El) F_1 hybrid mice were used as controls. Staged embryos are represented in the text by prefixing the embryological day with 'E'. Eyes from six different individuals were fixed overnight in Carnoy's fixative and transverse sections (2 μm) were stained with toluidine blue and basic fuchsin, mounted in Eukitt© (Kindler GmbH, Freiburg, Germany) and then processed for light microscopy (Klopp *et al*., 2001). Congo red- and haemotoxylin-counterstained lens tissue was viewed by either bright field (Stokes, 1976) or fluorescence (Linke, 2000) microscopy. Lens tissue was fixed in 1% (w/v) paraformaldehyde (PFA) buffered with 0.08 M phosphate buffer for several weeks. After alcohol dehydration, the lenses were embedded in Tecnovit® and 1–3 μm sections cut.

Immunolabelling and immunofluorescence microscopy

Mouse embryo samples were frozen immediately in liquid nitrogen. Lenses from at least five different animals were used for each experiment, and representative micrographs chosen. In the case of tissue culture cells, coverslips were washed in warm phosphate-buffered saline (PBS). Lens cryosections and tissue culture cells were then fixed in 4% (w/v) PFA and processed for immunofluorescence microscopy (Sandilands *et al*., 1995). Sections sometimes were counterstained with propidium iodide at a final concentration of 1 μg/ml to view chromatin. The Vector M.O.M. Immunodetection kit (Vector Laboratories, Cambridge, UK) was used to detect mouse monoclonal antibodies on mouse tissue.

Confocal images were collected with either a Zeiss LSM 410 unit (Carl Zeiss Ltd, Welwyn Garden City, Herts, UK) or a Biorad MRC 600 LSM (Biorad Laboratories, Ltd, Hemel Hempstead, Herts, UK). Digitally stored images were processed using Adobe Photoshop 5.

Primary antibodies

Mouse monoclonal antibodies to αA-crystallin (FitzGerald and Graham, 1991) were generously provided by Dr Paul Fitzgerald (Davis, CA). Actin monoclonal antibodies (AC40) were purchased from Sigma Chemical Co (Poole, UK). Rabbit polyclonal antibodies to CP49 (2981), vimentin (3052), αB-crystallin (3148) and γB^{nop}-crystallin have been described previously (Sandilands *et al*., 1995; Klopp *et al*., 1998). Rat polyclonal antibodies (Q1) to bovine filensin cross-reacted with mouse filensin (Carter *et al*., 1995). The specificity of secondary antibodies (Jackson ImmunoResearch Laboratories, Stratech Scientific Ltd, Luton, UK) was confirmed by staining samples in the absence of primary antibodies. Primary antibody specificity was confirmed by immunoblotting and by fluorescence microscopy after prior incubation with antigen, and also by comparison with pre-immune serum.

Expression constructs for γ-crystallins

Crygb was cloned by RT–PCR from mouse lens RNA using the forward (5′-TCAGCCATATGGGAAAGATC-3′) and reverse (5′-GAAAGTAG-AGTCTCAAAATGCC-3′) PCR primers. Amplified products were cloned into pGemTeasy (Promega), sequenced on both strands and then compared with the database entry (DDBJ/EMBL/GenBank accession No. Z22573). For bacterial expression, the cDNAs were subcloned into pET23b (Novagen, Nottingham, UK) and overexpressed in BL21(DE3) pLysS (Perng *et al*., 1999b). Proteins were purified using a Fractogel

EMD-DEAE anion exchange resin (Merck-BDH, Poole, UK). In some experiments, γ-crystallins were purified from wild-type mouse or bovine lenses by size exclusion chromatography (Nicholl and Quinlan, 1994).

For eukaryotic expression, *Crygb* and *Crygb^{nop}* were subcloned into the vector pEGFPC1 (Clontech Labs, Basingstoke, UK). Subconfluent PtK2 cells were transfected overnight with 4 μg of DNA using calcium chloride. Cells were allowed to recover for 24 h prior to processing for fluorescence and electron microscopy.

Lens extracts and immunoblotting

Whole eyes were collected from wild-type, heterozygous and homozygous *Crygb^{nop}* mice at E18.5 and were immediately extracted by homogenization in Laemmli's sample buffer (Laemmli, 1970) and then boiled. Protein concentrations were determined (Bradford, 1976), and equivalent protein loadings were analysed by SDS–PAGE. Proteins were transferred onto nitrocellulose (Merck-BDH, Poole, UK) and then blotted (Perng *et al*., 1999a).

Size exclusion chromatography

Samples were separated by size exclusion chromatography using a 100 × 1.0 cm Fractogel EMD BioSec650 column linked to a Merck-Hitachi bio-chromatography HPLC system. Eluting proteins were detected by monitoring absorbance at 280 nm. The column was run at 0.5 ml/min. Samples were separated using either 10 mM sodium phosphate pH 7.4, 100 mM KCl, 1 mM EDTA, or 50 mM Tris pH 7.4, 25 mM KCl, 5 mM $MgCl_2$. Elution times were calculated from the injection time to the mid-point of the relevant peak.

Amyloid fibril formation and characterization in vitro

Recombinant γB^{nop}-crystallin (0.5 mg/ml) was first dialysed into 8 M urea, 10 mM phosphate, 5 mM EDTA pH 8.0, and then dialysed into PBS over 24 h at room temperature via 4 M urea, 10 mM phosphate, 5 mM EDTA pH 8.0, followed by 10 mM phosphate, 5 mM EDTA pH 8.0. $A\beta_{1–40}$ (Sigma) was used as a positive control. Fibril formation was confirmed for each sample by negative staining and electron microscopy prior to further analysis.

For X-ray diffraction, a 10 μl aliquot of γB^{nop}-crystallin fibrils was suspended between two wax-filled capillary ends. The capillaries were separated slowly while drying using a stretch-frame apparatus to enhance alignment of amyloid fibrils in the fibre. A small stalk of fibrils protruding from the end of one of the capillaries was obtained. The fibre was aligned in an X-ray beam and diffraction images collected in a Cu-Kα rotating anode equipped with a 345 MAR-Research image plate (MAR Research, Hamburg, Germany). Images were analysed using MarView software.

Electron microscopy

For lenses or transfected cells, samples were fixed in 0.1 M cacodylate buffer containing 1.25% (v/v) glutaraldehyde and 1% (w/v) PFA, post-fixed with osmium tetroxide and then dehydrated in ethanol and embedded in epoxy resin before thin sectioning. Ultrathin sections were then contrasted with lead citrate and uranyl acetate and viewed in either a Philips CM12 or a Jeol 1200EX microscope. Images were captured on film, scanned at 1200 d.p.i. and assembled into figures using Adobe Photoshop.

Amyloid fibrils formed *in vitro* were diluted to 100–200 μg/ml and negatively stained using 1% (w/v) uranyl acetate. Grids were viewed in a Jeol 1200EX TEM, using an accelerating voltage of 80 kV.

Acknowledgements

The financial support of the Wellcome Trust is gratefully acknowledged by R.A.Q., A.R.P., A.M.H., C.M.D. and A.S. J.G. thanks the Deutsche Forschungsgemeinshaft (Gr 1036/4) for financial support. The project was also supported by an ARC project grant (1061) from the British Council to R.A.Q. and from the DAAD to J.G. (313-ARC-X). C.E.M. is a Royal Society Dorothy Hodgkin Research Fellow and should be contacted for the amyloid properties of Crygb^{nop}. H.A.L. is a BBSRC-funded student.

References

Bhat,S.P., Hale,I.L., Matsumoto,B. and Elghanayan,D. (1999) Ectopic expression of αB-crystallin in Chinese hamster ovary cells suggests a nuclear role for this protein. *Eur. J. Cell Biol.*, **78**, 143–150.

Bradford,M. (1976) A rapid and sensitive method for the quantitation of microgram quantities of protein utilizing the principle of protein–dye binding. *Anal. Biochem.*, **72**, 248–254.

Bruijn,L.I., Houseweart,M.K., Kato,S., Anderson,K.L., Anderson,S.D., Ohama,E., Reaume,A.G., Scott,R.W. and Cleveland,D.W. (1998) Aggregation and motor neuron toxicity of an ALS-linked SOD1 mutant independent from wild-type SOD1. *Science*, **281**, 1851–1854.

Bucciantini,M. *et al*. (2002) Inherent toxicity of aggregates implies a common mechanism for protein misfolding diseases. *Nature*, **416**, 507–511.

Carter,J.M., Hutcheson,A.M. and Quinlan,R.A. (1995) *In vitro* studies on the assembly properties of the lens beaded filament proteins: co-assembly with α-crystallin but not with vimentin. *Exp. Eye Res.*, **60**, 181–192.

Dahm,R., Gribbon,C., Quinlan,R.A. and Prescott,A.R. (1998) Changes in the nucleolar and coiled body compartments precede lamina and chromatin reorganization during fibre cell denucleation in the bovine lens. *Eur. J. Cell Biol.*, **75**, 237–246.

DiFiglia,M., Sapp,E., Chase,K.O., Davies,S.W., Bates,G.P., Vonsattel,J.P. and Aronin,N. (1997) Aggregation of huntingtin in neuronal intranuclear inclusions and dystrophic neurites in brain. *Science*, **277**, 1990–1993.

Dunah,A.W. *et al*. (2002) Sp1 and TAFII130 transcriptional activity disrupted in early Huntington's disease. *Science*, **296**, 2238–2243.

FitzGerald,P.G. and Graham,D. (1991) Ultrastructural localization of αA-crystallin to the bovine lens fiber cell cytoskeleton. *Curr. Eye Res.*, **10**, 417–436.

Foster,A. (1999) Cataract—a global perspective: output, outcome and outlay. *Eye*, **13**, 449–453.

Getzoff,E.D., Tainer,J.A., Stempien,M.M., Bell,G.I. and Hallewell,R.A. (1989) Evolution of CuZn superoxide dismutase and the Greek key β-barrel structural motif. *Proteins*, **5**, 322–336.

Graw,J. (1999) Mouse models of congenital cataract. *Eye*, **13**, 438–444.

Hatters,D.M., Lindner,R.A., Carver,J.A. and Howlett,G.J. (2001) The molecular chaperone, α-crystallin, inhibits amyloid formation by apolipoprotein C-II. *J. Biol. Chem.*, **276**, 33755–33761.

Head,M.W., Peter,A. and Clayton,R.M. (1991) Evidence for the extralenticular expression of members of the β-crystallin gene family in the chick and a comparison with δ-crystallin during differentiation and transdifferentiation. *Differentiation*, **48**, 147–156.

Heon,E., Priston,M., Schorderet,D.F., Billingsley,G.D., Girard,P.O., Lubsen,N. and Munier,F.L. (1999) The γ-crystallins and human cataracts: a puzzle made clearer. *Am. J. Hum. Genet.*, **65**, 1261–1267.

Horwitz,J. (1992) α-crystallin can function as a molecular chaperone. *Proc. Natl Acad. Sci. USA*, **89**, 10449–10453.

Hurle,M.R., Helms,L.R., Li,L., Chan,W. and Wetzel,R. (1994) A role for destabilizing amino acid replacements in light-chain amyloidosis. *Proc. Natl Acad. Sci. USA*, **91**, 5446–5450.

Ireland,M.E. *et al*. (2000) Up-regulation of novel intermediate filament proteins in primary fiber cells: an indicator of all vertebrate lens fiber differentiation? *Anat. Rec.*, **258**, 25–33.

Jacobson,D.R. and Buxbaum,J.N. (1991) Genetic aspects of amyloidosis. *Adv. Hum. Genet.*, **20**, 69–123.

Kegel,K.B. *et al*. (2002) Huntingtin is present in the nucleus, interacts with the transcriptional corepressor C-terminal binding protein and represses transcription. *J. Biol. Chem.*, **277**, 7466–7476.

Klopp,N. *et al*. (1998) Three murine cataract mutants (Cat2) are defective in different γ-crystallin genes. *Genomics*, **52**, 152–158.

Klopp,N., Löster,J. and Graw,J. (2001) Characterization of a 1-bp deletion in the γE-crystallin gene leading to a nuclear and zonular cataract in the mouse. *Invest. Ophthalmol. Vis. Sci.*, **42**, 183–187.

Kmoch,S. *et al*. (2000) Link between a novel human γD-crystallin allele and a unique cataract phenotype explained by protein crystallography. *Hum. Mol. Genet.*, **9**, 1779–1786.

Laemmli,U. (1970) Cleavage of structural proteins during the assembly of the head of bacteriophage T4. *Nature*, **277**, 680–685.

Lashuel,H.A., Wurth,C., Woo,L. and Kelly,J.W. (1999) The most pathogenic transthyretin variant, L55P, forms amyloid fibrils under acidic conditions and protofilaments under physiological conditions. *Biochemistry*, **38**, 13560–13573.

LeVine,H.,III (1999) Quantification of β-sheet amyloid fibril structures with thioflavin T. *Methods Enzymol.*, **309**, 274–284.

Linke,R.P. (2000) Highly sensitive diagnosis of amyloid and various amyloid syndromes using Congo red fluorescence. *Virchows Arch.*, **436**, 439–448.

McGowan,D.P., van Roon-Mom,W., Holloway,H., Bates,G.P., Mangiarini,L., Cooper,G.J., Faull,R.L. and Snell,R.G. (2000)

Amyloid-like inclusions in Huntington's disease. *Neuroscience*, **100**, 677–680.

Nicholl,I.D. and Quinlan,R.A. (1994) Chaperone activity of α-crystallins modulates intermediate filament assembly. *EMBO J.*, **13**, 945–953.

Pande,A., Pande,J., Asherie,N., Lomakin,A., Ogun,O., King,J. and Benedek,G.B. (2001) Crystal cataracts: human genetic cataract caused by protein crystallization. *Proc. Natl Acad. Sci. USA*, **98**, 6116–6120.

Pepys,M.B. (2001) Pathogenesis, diagnosis and treatment of systemic amyloidosis. *Philos. Trans. R. Soc. Lond. B Biol. Sci.*, **356**, 203–211.

Perng,M.D., Cairns,L., van den IJssel,P., Prescott,A., Hutcheson,A.M. and Quinlan,R.A. (1999a) Intermediate filament interactions can be altered by HSP27 and αB-crystallin. *J. Cell Sci.*, **112**, 2099–2112.

Perng,M.D., Muchowski,P.J., van den IJssel,P., Wu,G.J.S., Clark,J.I. and Quinlan,R.A. (1999b) The cardiomyopathy and lens cataract mutation in αB-crystallin compromises secondary, tertiary and quaternary protein structure and reduces *in vitro* chaperone activity. *J. Biol. Chem.*, **274**, 33235–33243.

Ray,M.E., Wistow,G., Su,Y.A., Meltzer,P.S. and Trent,J.M. (1997) AIM1, a novel non-lens member of the βγ-crystallin superfamily, is associated with the control of tumorigenicity in human malignant melanoma. *Proc. Natl Acad. Sci. USA*, **94**, 3229–3234.

Sandilands,A., Prescott,A.R., Carter,J.M., Hutcheson,A.M., Quinlan,R.A., Richards,J. and FitzGerald,P.G. (1995) Vimentin and CP49/filensin form distinct networks in the lens which are independently modulated during lens fibre cell differentiation. *J. Cell Sci.*, **108**, 1397–1406.

Santhiya,S.T., Shyam Manohar,M., Rawlley,D., Vijayalakshmi,P., Namperumalsamy,P., Gopinath,P.M., Löster,J. and Graw,J. (2002) Novel mutations in the γ-crystallin genes cause autosomal dominant congenital cataracts. *J. Med. Genet.*, **39**, 352–358.

Sisodia,S.S. (1998) Nuclear inclusions in glutamine repeat disorders: are they pernicious, coincidental, or beneficial? *Cell*, **95**, 1–4.

Stege,G.J., Renkawek,K., Overkamp,P.S., Verschuure,P., van Rijk,A.F., Reijnen-Aalbers,A., Boelens,W.C., Bosman,G.J. and de Jong,W.W. (1999) The molecular chaperone αB-crystallin enhances amyloid β neurotoxicity. *Biochem. Biophys. Res. Commun.*, **262**, 152–156.

Stokes,G. (1976) An improved Congo red method for amyloid. *Med. Lab. Sci.*, **33**, 79–80.

Suhr,S.T., Senut,M.C., Whitelegge,J.P., Faull,K.F., Cuizon,D.B. and Gage,F.H. (2001) Identities of sequestered proteins in aggregates from cells with induced polyglutamine expression. *J. Cell Biol.*, **153**, 283–294.

Teichmann,U., Ray,M.E., Ellison,J., Graham,C., Wistow,G., Meltzer, P.S., Trent,J.M. and Pavan,W.J. (1998) Cloning and tissue expression of the mouse ortholog of AIM1, a βγ-crystallin superfamily member. *Mamm. Genome*, **9**, 715–720.

Walsh,D.M., Klyubin,I., Fadeeva,J.V., Cullen,W.K., Anwyl,R., Wolfe,M.S., Rowan,M.J. and Selkoe,D.J. (2002) Naturally secreted oligomers of amyloid β protein potently inhibit hippocampal long-term potentiation *in vivo*. *Nature*, **416**, 535–539.

Warrick,J.M., Paulson,H.L., Gray-Board,G.L., Bui,Q.T., Fischbeck, K.H., Pittman,R.N. and Bonini,N.M. (1998) Expanded polyglutamine protein forms nuclear inclusions and causes neural degeneration in *Drosophila*. *Cell*, **93**, 939–949.

Wigle,J.T., Chowdhury,K., Gruss,P. and Oliver,G. (1999) Prox1 function is crucial for mouse lens-fibre elongation. *Nat. Genet.*, **21**, 318–322.

Wyttenbach,A., Sauvageot,O., Carmichael,J., Diaz-Latoud,C., Arrigo, A.P. and Rubinsztein,D.C. (2002) Heat shock protein 27 prevents cellular polyglutamine toxicity and suppresses the increase of reactive oxygen species caused by huntingtin. *Hum. Mol. Genet.*, **11**, 1137–1151.

Received July 25, 2002; revised September 18, 2002; accepted September 24, 2002